

## Synoptic Meteorology II: Contrasting the IPV and Quasi-Geostrophic Frameworks

**Readings:** No formal readings.

### **Introduction**

The quasi-geostrophic system of equations is a powerful system. As we demonstrated earlier in the semester, the quasi-geostrophic vorticity and height-tendency equations can be used to describe the motion and evolution of upper-tropospheric troughs and ridges. The quasi-geostrophic omega and Q-vector equations may be used to diagnose synoptic-scale vertical motion, while the latter may also be used to evaluate frontogenesis. The Petterssen-Sutcliffe development equation may be used to diagnose synoptic-scale surface cyclone development, motion, and evolution.

In recent weeks, we have introduced IPV, its mathematical formulation, and its conservation (or absence thereof). We described the structure of upper-tropospheric IPV and surface potential-temperature anomalies. We introduced how IPV, given an appropriate balance relationship or relationships, can be used to obtain the thermal and kinematic fields associated with a given IPV anomaly. Finally, we evaluated how diabatic heating and friction impact the three-dimensional IPV distribution.

To this point, however, we have *not* shown how IPV principles can be applied to describe the movement of the upper-tropospheric pattern, diagnose synoptic-scale forcing for vertical motion, or understand synoptic-scale surface cyclone development, motion, and evolution – all things we have done in the quasi-geostrophic system. Indeed, as we will demonstrate in this and the next lecture, IPV principles may be used to describe each of these concepts, thus highlighting how IPV “thinking” is a **complement** to quasi-geostrophic “thinking.”

### **The Movement of the Upper-Tropospheric Trough/Ridge Pattern**

Consider an atmosphere with no pre-existing relative vorticity ( $\zeta = 0$ ) and no background flow. We can express the IPV under such conditions as:

$$P = -gf \frac{\partial \theta}{\partial p} \quad (1)$$

Since  $f$  increases in magnitude with increasing latitude,  $P$  is larger in magnitude toward the poles and smaller in magnitude toward the equator. This is depicted in Fig. 1.



**Figure 1.** Horizontal distribution of  $P$  resulting exclusively from meridional variability in the Coriolis parameter  $f$ .

Let us superimpose a series of alternating positive and negative upper-tropospheric IPV anomalies on the distribution of  $P$  highlighted in Fig. 1. The result of doing so at the latitude where  $P = P$  is depicted in Fig. 2.

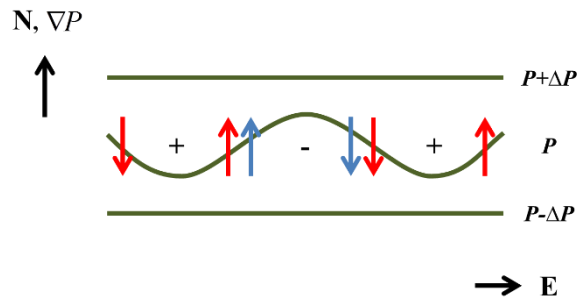


**Figure 2.** Horizontal distribution of  $P$  resulting from the superposition of the meridional variability in the Coriolis parameter  $f$  and a series of alternating positive and negative upper-tropospheric IPV anomalies. The flow associated with these anomalies is depicted by red and blue arrows, respectively.

By definition, positive upper-tropospheric IPV anomalies are associated with cyclonic flow and negative upper-tropospheric IPV anomalies are associated with anticyclonic flow. These flows are depicted by blue and red arrows, respectively, in Fig. 2.

The advection of  $P$  by these flows results in positive  $P$  advection to the west of a positive IPV anomaly and negative  $P$  advection to the west of a negative IPV anomaly. This results in the

*westward* movement of the upper-tropospheric trough/ridge pattern associated with the alternating positive and negative upper-tropospheric IPV anomalies!

Earlier this semester, we demonstrated that the relative strength of the wind field  $U$  associated with a given IPV anomaly is directly proportional to that anomaly's horizontal length scale  $L$ :

$$U = \sigma_{ref}^* PL \quad (2)$$

IPV anomalies of greater horizontal extent (larger  $L$ ) are associated with stronger wind fields and IPV anomalies of lesser horizontal extent (smaller  $L$ ) are associated with weaker wind fields. As a result, the westward propagation described above is more rapid for larger-scale IPV anomalies (e.g., longwaves) and less rapid for smaller-scale IPV anomalies (e.g., shortwaves).

Finally, let us impose a background westerly flow in our example. The combination of the westerly flow and the westward motion of the pattern that results from IPV advection allows us to state:

- Larger-scale (longwave) troughs retrogress to the west against the large-scale flow or move eastward at a relatively slow rate of speed; i.e., the advection of IPV associated solely with the meridional variation in the Coriolis parameter dominates.
- Shortwave troughs move to the east at a rate of speed that is equal to or somewhat less than that of the large-scale westerly flow; i.e., the advection of IPV by the background flow dominates.

These insights match those of the geostrophic relative-vorticity advection and planetary vorticity advection forcing terms contained in the quasi-geostrophic vorticity equation!

### **Surface Cyclone and Anticyclone Movement**

The conceptual framework for understanding surface cyclone and anticyclone movement is very similar to that for the upper-tropospheric pattern, except we consider the background meridional potential-temperature distribution here (consistent with our discussion of surface IPV anomalies). On level terrain and in the absence of non-radiative diabatic processes, the background potential-temperature distribution at the surface is largely determined by the meridional distribution of solar insolation. Areas near the Equator are warmer because they receive greater solar insolation, while areas near the poles are colder because they receive lesser solar insolation. The resulting background potential-temperature distribution at the surface is depicted in Fig. 3.



**Figure 3.** The meridional potential-temperature distribution due to meridional variability in solar insolation.

Superimpose a series of alternating warm and cold surface potential-temperature anomalies upon the  $\theta$  distribution in Fig. 3. The result of doing so along the latitude where  $\theta = \theta$  is depicted in Fig. 4.

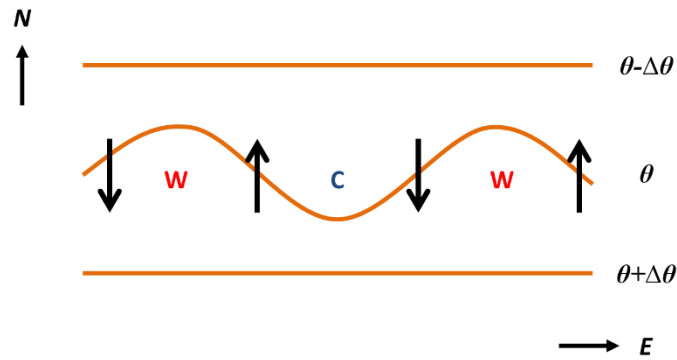


**Figure 4.** The meridional potential-temperature distribution that results from the superposition of the distribution depicted in Fig. 3 with a series of alternating warm and cold surface potential-temperature anomalies. The flow associated with these anomalies is depicted by the black arrows.

Before, we found that warm (positive) surface potential-temperature anomalies are akin to positive upper-tropospheric IPV anomalies and cold (negative) surface potential-temperature anomalies are akin to negative upper-tropospheric IPV anomalies. Thus, warm surface potential-temperature anomalies are associated with cyclonic flow and cold surface potential-temperature anomalies are associated with anticyclonic flow. This is depicted by the arrows in Fig. 4.

Potential-temperature advection by the induced cyclonic and anticyclonic vortices results in positive potential-temperature advection east of warm surface potential-temperature anomalies

and negative potential-temperature advection east of cold surface potential-temperature anomalies. As a result, surface cyclones and anticyclones move *eastward*. This is the same insight that we drew from the thermal advection term in the Petterssen-Sutcliffe development equation: surface cyclones move toward areas of lower-tropospheric warm advection (e.g., toward areas of cyclone development) and surface anticyclones move toward areas of lower-tropospheric cold advection (e.g., away from areas of cyclone development).

### Diagnosing Vertical Motion with Upper-Tropospheric IPV Anomalies

Consider a positive upper-tropospheric IPV anomaly embedded in westerly vertical wind shear, as depicted in Fig. 5. Note that similar arguments to the ones that we will make below can be made for positive and negative upper-tropospheric IPV anomalies in any vertically sheared environment.

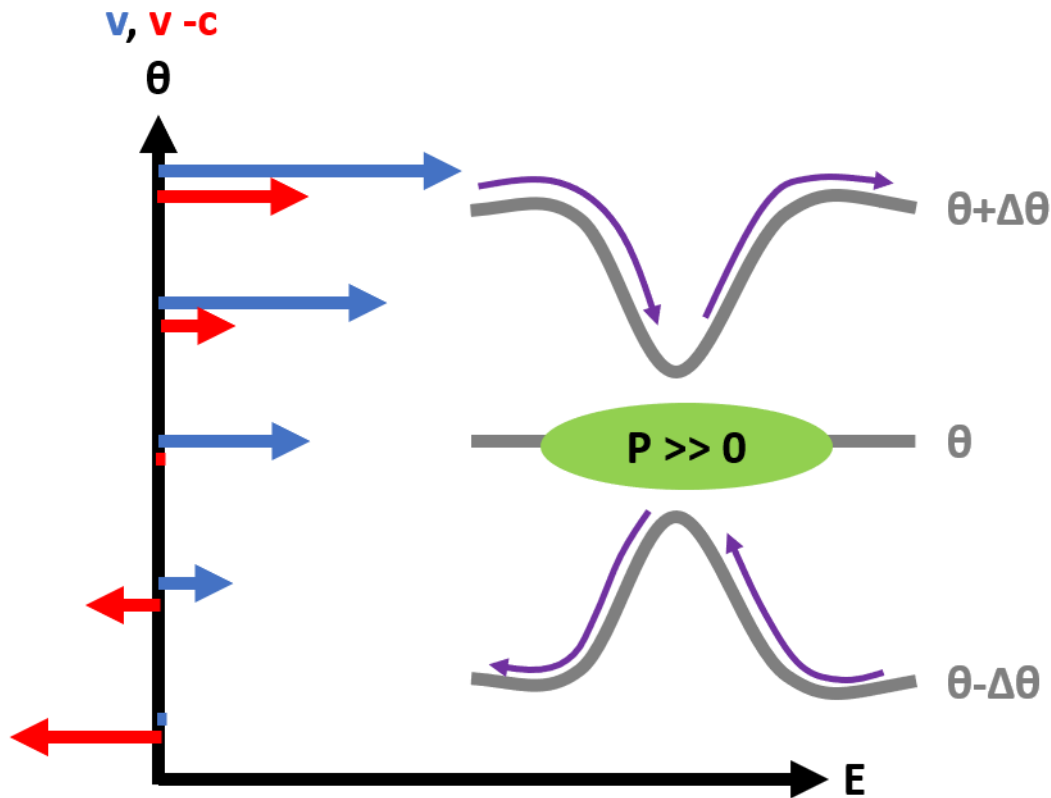


**Figure 5.** Vertical cross-section depicting a positive upper-tropospheric IPV anomaly (green oval), isentropes (grey lines), the synoptic-scale (blue arrows) and system-relative (red arrows) wind, and isentropic flow corresponding to the system-relative wind (purple arrows).

Consider a reference frame that moves with the positive upper-tropospheric IPV anomaly. Assume that the positive upper-tropospheric IPV anomaly moves eastward with the layer-mean wind. Subtracting its motion from the wind at each level depicted in Fig. 5, we obtain a system-relative easterly flow that decreases with increasing height. This is depicted by the red arrows on the left-hand side of Fig. 5.

Assume that potential temperature does not change following the motion (i.e., purely adiabatic flow). In the reference frame moving with the positive IPV anomaly, that motion is the system-relative motion. Thus, above the level at which the positive IPV anomaly is most intense, this motion is westerly (i.e., the air moves faster to the east than does the IPV anomaly). Below the level at which the positive IPV anomaly is most intense, this motion is easterly (i.e., the air moves slower to the east than the IPV anomaly). Together, these imply ascent to the east and descent to the west of the positive IPV anomaly. This is akin to the differential geostrophic advection of geostrophic absolute vorticity forcing term in the quasi-geostrophic omega equation.

Further, from thermal-wind principles, the positive IPV anomaly embedded in westerly vertical wind shear is associated with a north-south layer-mean temperature gradient with colder air to the north and warmer air to the south. This implies that the isentropes depicted in Fig. 5 will slope upward toward the north and downward toward the south. The cyclonic flow associated with the positive IPV anomaly is directed from south to north to the east, such that an air parcel conserving its potential temperature will ascend along the upward-sloped isentrope. Conversely, the cyclonic flow is directed from north to south to the west, such that an air parcel conserving its potential temperature will descend along the downward-sloped isentrope. This is akin to the Laplacian of potential-temperature advection forcing term in the quasi-geostrophic omega equation.

Together, the insight garnered using the IPV framework and principles of isentropic analysis is identical to that obtained from the quasi-geostrophic system.

### **Diagnosing Vertical Motion with Surface Potential-Temperature Anomalies**

The logic introduced in the previous section for upper-tropospheric IPV anomalies also applies to surface potential-temperature anomalies.

A warm surface potential-temperature anomaly in a westerly sheared environment has the same structure as that of the upper-half of the positive IPV anomaly in Fig. 5. Consequently, the insight garnered above is also applicable here: system-relative flow is from west to east, implying ascent to the east and descent to the west.

A cold surface potential-temperature anomaly in a westerly sheared environment has the opposite structure to that of the upper-half of the positive IPV anomaly in Fig. 5. While the system-relative flow is again from west to east, flow along the upward-bowing isentropes in this case implies descent to the east and ascent to the west.